Functional domains of interferon regulatory factor I (IRF-1)

Fred SCHAPER*[1], Sabine KIRCHHOFF*, Guido POSERN*[2], Mario KÖSTER*, André OUMARD*, Rakefet SHARF†, Ben-Zion LEVI† and Hansjörg HAUSER*[3]

*Gesellschaft für Biotechnologische Forschung mbH, Mascheroder Weg 1, 38124 Braunschweig, Federal Republic of Germany, and †Technion, Israel Institute of Technology, Haifa 32000, Israel

Interferon (IFN) regulatory factors (IRFs) are a family of transcription factors among which are IRF-1, IRF-2, and IFN consensus sequence binding protein (ICSBP). These factors share sequence homology in the N-terminal DNA-binding domain. IRF-1 and IRF-2 are further related and have additional homologous sequences within their C-termini. Whereas IRF-2 and ICSBP are identified as transcriptional repressors, IRF-1 is an activator. In the present work, the identification of functional domains in murine IRF-1 with regard to DNA-binding, nuclear translocation, heterodimerization with ICSBP and transcriptional activation are demonstrated. The minimal DNA-binding domain requires the N-terminal 124 amino acids plus an arbitrary C-terminal extension. By using mutants of IRF-1 fusion proteins with green fluorescent protein and monitoring their distribution in living cells, a nuclear location signal (NLS) was identified and found to be sufficient for nuclear translocation. Heterodimerization was confirmed by a two-hybrid system adapted to mammalian cells. The heterodimerization domain in IRF-1 was defined by studies *in vitro* and was shown to be homologous with a sequence in IRF-2, suggesting that IRF-2 also heterodimerizes with ICSBP through this sequence. An acidic domain in IRF-1 was found to be required and to be sufficient for transactivation. Epitope mapping of IRF-1 showed that regions within the NLS, the heterodimerization domain and the transcriptional activation domain are exposed for possible contacts with interacting proteins.

INTRODUCTION

Interferon (IFN) regulatory factor (IRF)-1 was identified as a transcriptional activator of the *IFN-β* gene by binding to positive regulatory domain I and positive regulatory domain III within the promoter [1–4]. IRF-1 is also able to activate transcription of certain IFN-stimulated genes by binding to IFN-stimulated response elements (ISREs). The core sequences of these responsive elements are similar to the positive regulatory domain I of the IFN-*β* promoter. IRF-1 expression is induced by viruses, IFNs, a number of cytokines such as interleukin-1, tumour necrosis factor, platelet-derived growth factor and colony-stimulating factor. The promoter of the *IRF-1* gene contains elements, including IFN-*γ*-activated sequences, and binding sites for SP1 and nuclear factor-*κ*B. IRF-1 overexpression leads to an antiproliferative state of the cell and to apoptosis under certain circumstances [5–7]. This activity is independent of its ability to induce IFNs but requires the DNA binding and transcriptional activity [5]. Furthermore, IRF-1 has been identified as a tumour suppressor [2,7,8]. It co-operates with the tumour suppressor p53 in response to DNA damage and shows a functional homology with p53 [9].

Functional antagonists of IRF-1 are IRF-2 and IFN consensus sequence binding protein (ICSBP) [3,10–12]. IRF-2 represses the IFN-*β* promoter activity constitutively. Virus induction leads to the replacement of IRF-2 by IRF-3 [13]. ICSBP is also an ISRE binding protein and a member of the IRF family. It is induced in haematopoietic cells by IFN-*γ* but not by IFN-*α* or -*β* [14]. ICSBP has been shown to repress IFN- and IRF-1-mediated activation of ISRE-driven genes [10,12]. Functional assays showed that ICSBP is an antagonist of IRF-1 transactivation [10–12,15]. The C-terminus of ICSBP contains a transcriptional repressor domain. This domain can be functionally separated from the DNA-binding activity of ICSBP and therefore acts independently of the ICSBP DNA-binding function [15]. ICSBP interacts physically with IRF-1 and IRF-2 in assays *in vitro* [15–17]. Although the heterodimerization of ICSBP with IRF-1 (and IRF-2) has been demonstrated, the mechanism of this repression is not understood [11,16,17]. However, the interaction might be of major importance for the homoeostasis of the cellular proliferation state, since mice lacking ICSBP develop a syndrome which is similar to chronic myelogenous leukaemia [18].

To elucidate the functions and mechanisms of IRF-1 action we defined functional domains of IRF-1. In the present work, we have shown the heterodimerization of IRF-1 with ICSBP in a mammalian cell two-hybrid system and identified the responsible domain in IRF-1. We have identified the nuclear location signal (NLS) of IRF-1 and localized, in greater detail, the regions which contribute to, and which are sufficient for, transcriptional activation and DNA binding.

EXPERIMENTAL

Plasmid constructions

Constructions were carried out by standard procedures [19]. pMT7IRF-1 [5] contains the cDNA of the murine IRF-1 gene under the control of the MT7 promoter [20]. pMBC-1-green fluorescent protein (GFP), a PCR product coding for GFP, was inserted into pMBC-1 [21]. The MT7 promoter within these

Abbreviations used: CAT, chloramphenicol acetyltransferase; EMSA, electromobility-shift assay; IFN, interferon; GAL, galactosidase; GFP, green fluorescent protein; ICSBP, IFN consensus-sequence binding protein; IRF, interferon regulatory factor; ISRE, IFN-stimulated response element; NLS, nuclear location signal; hER, human oestrogen receptor.

[1] Present address: Institut J. Biochemie, Klinikum d. RWTH Aachen, Pauwelstr. 30, 52074 Aachen, Germany.

[2] Present address: Universität Würzburg, Institute for Medical Radiation and Cell Research, Versbacher Straße 5, 97078 Würzburg, Federal Republic of Germany.

[3] To whom correspondence should be addressed (e-mail hha@gbf-braunschweig.de).

constructs allows expression in mammalian cells and transcription with T7-RNA polymerase *in vitro* [20]. pMBC-1–IRF-1–GFP was generated by fusing a PCR product, coding for the cDNA of GFP with the C-terminus of the murine IRF-1 cDNA integrated into pMBC-1. In pMBC-1–M6-GFP, the IRF-1 coding DNA fragment of pMBC-1–IRF-1–GFP was replaced by the IRF-1 DNA fragment of pMT7-M6 [5], coding for an IRF-1 protein which lacks amino acids 2–34. In pMBC-1–Δbasic-GFP, the IRF-1-encoding DNA fragment of pMBC-1–IRF-1–GFP was replaced by a PCR product coding for an IRF-1 mutant in which amino acids 116–139 were exchanged for Gly-Ala. In pMBC-1–basic GFP, the IRF-1-encoding DNA fragment of pMBC-1–IRF-1–GFP was replaced by a PCR product coding for a methionine initiation codon and the amino acids 117–141 of IRF-1. In pMBC-1–Δacid (Δ221–255), the IRF-1-encoding DNA fragment of pMBC-1–IRF-1 was replaced by a PCR product coding for an IRF-1 mutant in which amino acids 221–255 were replaced by Gly-Ala. In pMBC-1-Δ221-231, the IRF-1-encoding DNA fragment of pMBC-1–IRF-1 was replaced by a PCR product coding for an IRF-1 mutant in which amino acids 221–231 were replaced by Gly-Ala. In pMBC-1–Δ190-216, the DNA fragment of pMBC-1–IRF-1 coding for IRF-1 was replaced by a PCR product coding for a mutant of IRF-1 in which amino acids 190–216 were replaced by Gly-Ala. In pMT7–VP16, a PCR product coding for amino acids 412–490 of the VP16 protein was integrated into pMT7HE with its own ATG initiation codon. pSGMT7 was generated by replacing the simian virus (SV)-40 promoter of pSG424 by the MT7 promoter from pMT7HE [21]. pSGMT7–IRF-1 was generated by integrating the DNA fragment for IRF-1 in frame to galactosidase (GAL)4 in pSGMT7. In pSGMT7–Δ221-255, the IRF-1-encoding DNA fragment of pSGMT7–IRF-1 was replaced by a PCR product coding for an IRF-1 mutant in which amino acids 221–255 were replaced by Gly-Ala. In pSGMT7–Δ221-231, the IRF-1-encoding DNA fragment of pSGMT7–IRF-1 was replaced by a PCR product coding for an IRF-1 mutant in which amino acids 221–231 were replaced by Gly-Ala. In pSGMT7–Δ190-216, the IRF-1-encoding DNA fragment of pSGMT7–IRF-1 was replaced by a PCR product coding for an IRF-1 mutant in which amino acids 190–216 were replaced by Gly-Ala. In pSGMT75,6, the IRF-1-encoding DNA fragment of pSGMT7–IRF-1 was replaced by a PCR product coding for an IRF-1 fragment coding for amino acids 185–220. In pSGacid, the ICSBP-encoding DNA fragment of pSGICSBP was replaced by a PCR product coding for an IRF-1 fragment encoding amino acids 185–220. pSGICSBP encodes for a fusion protein of the GAL4 DNA-binding domain and ICSBP [15]. pMT7–IRF-1–VP16 was generated by the replacement of the human oestrogen receptor (hER) DNA fragment of pMT7–IRF-1–hER [5] in frame by a PCR product coding for amino acids 412–490 of the VP16 protein. pMT7-M6-VP16 was generated by the replacement of the hER DNA fragment of pMT7–M6–hER [5] in frame by a PCR product coding for amino acids 412–490 of the VP16 protein. pMT7–Hetero-VP16 was generated by replacing the IRF-1-encoding DNA fragment of pMT7–IRF-1–VP16 by a PCR product coding for the amino acids 164–219 of IRF-1. pMCM13 [15,19,22] contains the chloramphenicol acetyltransferase (CAT) gene controlled by a GAL4-responsive promoter construct. pBHELuc has been described earlier [23].

Expression of IRF-1 derivates *in vitro*

Templates for *in vitro* run-off transcription/translation were generated by integration of the coding DNAs into vectors containing the MT7 promoter (pMT7, or pMBC-1) [20,21] and linearization downstream of the coding region. Alternatively, the templates were generated by PCR using a 5′ primer containing the T7 promoter. Both methods for template generation lead to the same results (compare Figure 1B, lanes 2 and 4). The IRF-1 mutants were: 1-273, amino acids 1–273; 1-247, amino acids 1–247; 1-219, amino acids 1–219; 1-198, amino acids 1–198 [5]; 1-174, amino acids 1–174 of IRF-1; 1-142, the randomized amino acid sequence MLARTLSLMDSAALPYLMTTAVTPLRAT was fused C-terminally to the N-terminal amino acids 1–142 of IRF-1; 1-86, ALPAHHHHHHT was added to the N-terminal amino acids 1–86 of IRF-1; FS143-163, amino acids 143–163 were replaced by ^{143}MLARTLSLMDSAALPYLMTTAV; 35-329 (= M6), deletion of amino acids 2–34 [21]; 65-329, deletion of amino acids 2–64; 115-329, deletion of amino acids 2–114; Δ115-140 (= Δbasic), replacement of amino acids 115–139 by Gly-Ala; Δ125-140, replacement of amino acids 125–140 by GlyAla; Δ221-255 (= Δacid), replacement of amino acids 221–255 by Gly-Ala; Δ190-216, replacement of amino acids 190–216 by Gly-Ala.

Run-off RNA was produced using the T7 RNA polymerase (Boehringer/Mannheim) in the presence of m^{7}GpppG. RNA synthesis was quantified by incorporation of [α-^{32}P]GTP (Amersham). For the production of recombinant protein in rabbit reticulocyte lysates (Promega), 50–100 ng of RNA was used. Each translation experiment was carried out twice, once in the presence of ^{35}S-labelled methionine to control translation efficiency, the other with unlabelled methionine. The translation procedure was performed according to the manufacturer's instructions. The radioactive proteins were separated on polyacrylamide gels overnight at 90 V, fixed in 2-propanol/acetic acid/water (5:2:13, by vol.), dried and autoradiographed. ^{14}C-Labelled protein standards (Gibco) were used to identify the mass of the synthesized proteins.

Electromobility-shift assays (EMSA)

The indicated proteins were translated in the rabbit reticulocyte lysate *in vitro*. For testing heterodimerization, lysates containing the different proteins were mixed. EMSA analysis was carried out according to the protocol of Fried and Crothers [24]. Proteins were incubated with 20000 c.p.m. of labelled 5′-GATCCTCGGGAAAGGGAAACCGAAACTGAAGCC-3′ (IFN-stimulated gene 15-ISRE [2]) or the T3 DNA fragment, 5′-AAGTGAAAGTGAAAGTGA-3′ (positive regulatory domain I of the IFN-β promoter), in the presence of 1 μg of poly[d(I,C)] and 2 μg of herring sperm DNA in 10 mM Hepes pH 8.0/5 mM $MgCl_2$/50 mM KCl/0.5 mM dithiothreitol/0.005% (w/v) Bromphenol Blue/0.005% (w/v) Xylene Cyanol and 2% (w/v) Ficoll. The samples were loaded on pre-electrophoresed 6% (w/v) polyacrylamide Tris/borate gels. After drying, the gels were autoradiographed. For supershift assays (see Figure 5) 1–5 μl of antibody were added to the sample.

Immunological techniques

Epitope mapping was performed as described by Frank [25]. Polyclonal antibodies raised against peptides of murine IRF-1 in rabbits were produced by EuroGentec (Brussels, Belgium). For immunoprecipitation, IRF-1 was translated in rabbit reticulocyte lysate in the presence of [^{35}S]methionine. The translation product (10 μl) was incubated with 2 μl of antiserum with peptides at 4 °C for 2 h. Protein G-Sepharose (Pharmacia) (20 μl) was added and incubation was continued for 2 h. After centrifugation, the Protein G-Sepharose was washed 5 times with 500 μl of NET-NON [500 mM NaCl/5 mM EDTA/50 mM Tris/HCl, pH 8.0/

0.5 % (v/v) NP-40/0.05 % sodium azide containing 1 mg/ml of ovalbumin]. Sample buffer (50 μl) was added and the Protein G-Sepharose was heated to 65 °C for 5 min. Aliquots of the supernatant (25 μl) were subjected to SDS/PAGE [26]; the gels were fixed in 2-propanol/acetic acid (5:2, v/v), dried and autoradiographed.

For determination of GAL4 fusion protein levels, Western blots of cellular extracts from transiently transfected cells were prepared and probed with a polyclonal antibody directed against GAL4 protein. The blots were revealed by enhanced chemiluminescence (Amersham) according to the manufacturer's instructions.

Cell culture and gene transfer

Mouse fibroblastoid C243 cells [27,28] were maintained in Dulbecco's modified Eagle's medium with 10 % (v/v) fetal-calf serum, 100 units/ml of ampicillin, 0.1 mg/ml of streptomycin and 292 mg/l of glutamine. DNA (1μg of effector DNA, 1 μg of reporter DNA, 1 μg of luciferase-encoding DNA and 2 μg of high-molecular-mass DNA) was transfected using calcium phosphate co-precipitation for 1×10^5 cells/18-cm^2 plate [29]. The medium was changed 4 h before transfection and renewed 20 h after transfection. Cells were harvested 48 h after transfection.

For two-hybrid assays, the GAL-fusion-protein-encoding plasmid was used in constant amounts (0.5 μg), whereas the VP16-fusion-protein-encoding plasmid was titrated up to 4-fold of the GAL-fusion-protein-encoding plasmid. The total amount of plasmids was adjusted to a constant level (5 μg), with control plasmids coding for the VP16 transactivation domain alone.

Reporter gene assays

CAT analyses were performed using CAT–ELISA (Boehringer-Mannheim) according to the manufacturer's instructions. Extracts were prepared from transfected cells by freezing and thawing. Luciferase activity was measured as described by de Wet et al. [30]. In transient expression experiments, the CAT amount was normalized to the protein concentration. Luciferase co-expression was used to prove DNA transfer (pBHELuc [30]). The results shown are based on more than three independent transfection experiments.

RESULTS

Nuclear translocation

As a transcriptional activator IRF-1 is expected to reside in the nucleus. Sequences for nuclear location signals (NLS) contain a stretch of lysines (K) and arginines (R) and are usually located at accessible positions in the protein for interacting with NLS-binding proteins (for review see [31]). IRF-1 contains two such potential sequences which might act as NLS, ^{120}RKERKSK and ^{132}KSKTKRK. In the present study an attempt was made to identify the sequence which is required and is sufficient to translocate IRF-1 from the site of synthesis in the cytoplasm to the nucleus.

To demonstrate the nuclear localization of IRF-1, indirect immunofluorescence was used to detect endogenous IRF-1 protein. With the available antibody it was not possible to visualize endogenous IRF-1 unambiguously. Therefore IRF-1 tagged with the haemagglutinin epitope was overexpressed and its localization exclusively to the nucleus was determined (Figure 1A). To identify the position of the IRF-1 NLS, a number of IRF-1 mutants as green fluorescent fusion proteins were prepared (Figure 2). GFP [32] offers a number of advantages for this purpose: (i) because of the high sensitivity for detection only a small amount of the tagged protein is needed, thereby reflecting conditions of the endogenous protein; (ii) *in vivo* detection allows the localization of the tagged protein in living cells, thus avoiding fixation artifacts; (iii) as a full-length protein, GFP can be used as an acceptor for peptide location sequences (e.g. the NLS); (iv) wild-type GFP has no distinct localization in higher mammalian cells. Due to unhindered diffusion, it is found in the cytoplasm as well as in the nucleus (see Figure 1F), but localization sequences pull GFP to different subcellular compartments [33].

A number of mutants and fusion proteins with GFP was tested. The most important ones are shown in Figure 2. The wild-type GFP protein was found in the nucleus as well as in the cytoplasm (Figure 1F). The fusion protein IRF-1–GFP, consisting of IRF-1 fused to GFP, was found in the nucleus (Figure 1B). The mutant of IRF-1 lacking both potential NLS (amino acids 116–139) fused to GFP (Δbasic-GFP) was localized in the cytoplasm (Figure 1C), indicating that amino acids 116–139 are essential for nuclear localization. This IRF-1 mutant did not bind DNA (see below). In order to show that the nuclear location of IRF-1 was not linked to its DNA binding activity, another non-DNA-binding mutant of IRF-1 (M6 [20]) was tested as a GFP fusion protein. This mutant, M6–GFP, lacks the 34 N-terminal amino acids. The M6–GFP protein was also found in the nucleus (Figure 1D). To examine whether the basic domain containing the NLS is sufficient for nuclear translocation, a construct in which amino acids 117–141 were fused to GFP (basic-GFP) was used. This protein was localized to the nucleus (Figure 1E). It was concluded, from these results, that the NLS was contained within the amino acid sequence 117–141. Furthermore, this sequence was sufficient to direct a heterologous protein (GFP) without endogenous NLS into the nucleus.

Heterodimerization with ICSBP

The mechanism for the antagonistic activity of ICSBP and IRF-1-induced gene activation is still unknown. Since competition for DNA-binding sites is not sufficient to explain the antagonistic effect of ICSBP [15], we speculate that an interaction of both proteins gives rise to a transcriptional inactive DNA-binding complex.

To demonstrate that a physical interaction between IRF-1 and ICSBP takes place *in vivo*, a two-hybrid system adapted for mammalian cells was used. This system was validated previously by monitoring the dimerization of p50 as GAL–p50 and p50–VP16 fusion proteins. Co-expression of both fusion proteins resulted in a 10-fold stimulation of a GAL4-responsive reporter construct (pMCM13) (S. Kirchhoff, F. Schaper, A. Oumard and H. Hauser, unpublished work).

Fusion proteins consisting of the DNA-binding domain of the yeast GAL4 protein and ICSBP, of which 33 N-terminal amino acids were deleted to disrupt their DNA-binding domain (GAL–ICSBP), were tested in this assay. This GAL–ICSBP protein interacted with a fusion protein composed of IRF-1 and the transcriptional activation domain of the herpes simplex virus VP16 protein (IRF-1–VP16) in transiently transfected C243 fibroblasts. This interaction was monitored by a CAT-reporter construct driven by a GAL4-responsive promoter. The results of the mammalian two-hybrid system are summarized in Table 1. GAL4- and VP16-encoding constructs, single or co-expressed, did not induce CAT activity. The GAL–ICSBP fusion protein does not bind ISRE elements since it lacks amino acids 1–33 from ICSBP. However, GAL–ICSBP can bind the GAL4-responsive promoter through its GAL4 DNA-binding domain. The IRF-1 mutant M6 does not bind to the endogenous ISRE

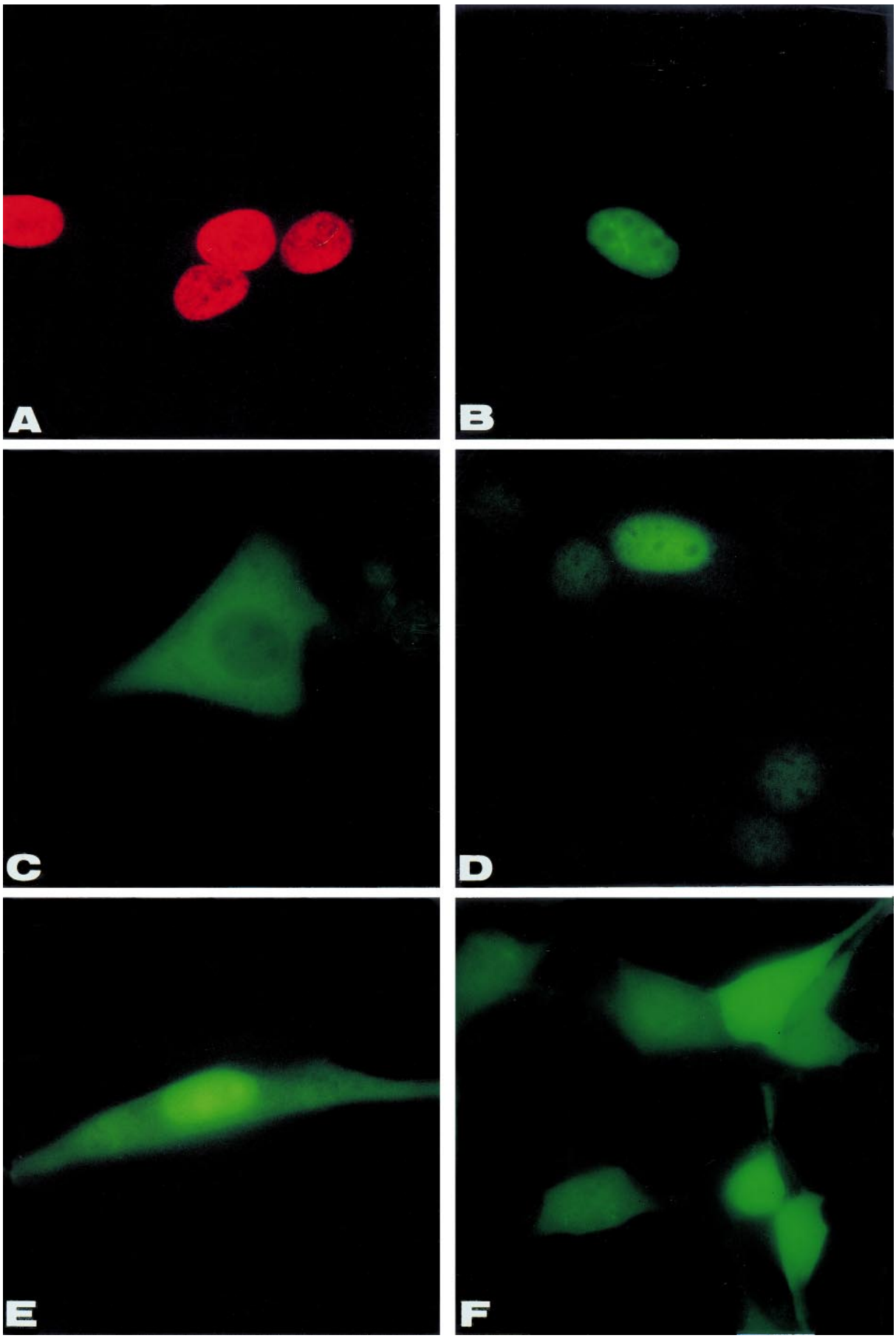
A
B
C
D
E
F

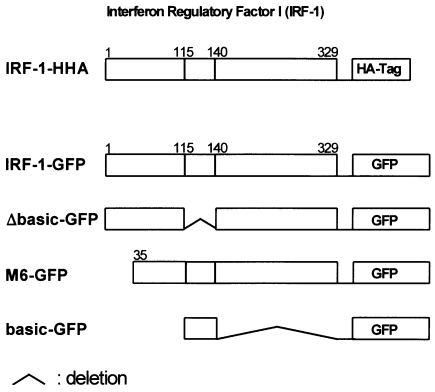

Figure 2 Tagged IRF-1 constructs

The box diagrams show the GFP constructs used for transfections used in Figure 1. The indicated deletions resulted in in-frame fusions of the hybrid proteins (see the Experimental section). The numbering corresponds to amino acids in the wild-type IRF-1.

Table 1 Heterodimerization in the mammalian two-hybrid system

Expression vectors coding for fusion proteins containing the DNA-binding domain of the GAL4 transcription factor and ICSBP (lacking the N-terminal 33 amino acids) (GAL-ICSBP) or the GAL4 DNA-binding domain alone (GAL) were cotransfected with vectors encoding the transactivation domain of the herpes simplex virus VP16 transcription factor (VP16) or fusion proteins of the latter with IRF-1 proteins. (IRF-1, full length IRF-1; M6, IRF-1 lacking the 34 N-terminal amino acids; 125-219-VP16, amino acids 125–219 of IRF-1 fused to the VP16 transactivation domain.) The induction of the co-transfected GAL-dependent reporter construct was measured at the CAT protein level. Induction levels (CAT activity) were normalized to the corresponding control experiments with the GAL4 DNA-binding domain. Data are given as means ± S.E.M. of at least three independent experiments.

Protein A[a]	Protein B[b]	CAT activity
GAL	–	1
–	VP16	0.8 (±0.4)
GAL	VP16	0.8 (±0.4)
GAL-ICSBP	–	1.1 (±0.2)
–	IRF-1-VP16	0.9 (±0.2)
–	M6-VP16	0.9 (±0.1)
GAL-ICSBP	IRF-1-VP16	3.2 (±0.7)
GAL-ICSBP	M6-VP16	3.7 (±0.9)
GAL-ICSBP	–	1.1 (±0.2)
GAL-ICSBP	125-219-VP16	0.9 (±0.5)

[a] DNA-binding protein.
[b] Transactivating protein.

elements; therefore, the fusion protein M6–VP16 consisting of M6 and the VP16 transactivation domain was constructed. Upon expression in C243 cells, none of the three fusion proteins GAL–ICSBP, IRF-1–VP16 or M6–VP16 induced the reporter construct pMCM13. Co-transfection of GAL–ICSBP together with IRF-1–VP16 or GAL–ICSBP with M6–VP16 resulted in induction of the reporter gene (Table 1). These experiments clearly prove heterodimerization between ICSBP and IRF-1 in living cells.

To define the IRF-1 domain, which is responsible for interaction with ICSBP, an *in vitro* heterodimerization assay was used which allowed a large number of IRF-1 mutants to be tested in a simple, reliable and rapid manner. The mutant IRF-1 proteins developed for this experiment are shown in Figure 3 (upper panel). These IRF-1 proteins and ICSBP were translated in a rabbit reticulocyte lysate in the presence or absence of [^{35}S]methionine. The radiolabelling experiments were used to control translation efficiency of mutant proteins (results not shown). The [^{35}S]methionine content of the IRF-1 mutant proteins were quantified and corrected for methionine content. Translation efficiency was found to be similar for all proteins (relative efficiency is given in legend to Figure 3, lower panel). The unlabelled proteins were used in the heterodimerization assay *in vitro*. IRF-1 translated in rabbit reticulocyte lysate binds to the positive-regulatory-domain-I-related sequence $(AAGTGA)_3$ [5], as well as to the ISRE of the IFN-stimulated-gene-15 gene promoter [16] (Figure 3 lower panel; lanes 2, 4 and 24). As shown previously, *in vitro* translated ICSBP does not bind to target DNA [15,17]. Therefore ICSBP was not visible in this assay (Figure 3 lower panel, lane 26). A mixture of separately translated IRF-1 and ICSBP produced additional retardation (lanes 3, 5 and 25). This is consistent with the formation of ICSBP–IRF-1 heterodimers [16,17].

In order to identify the domain in IRF-1 responsible for heterodimerization with ICSBP, a supershift assay was used to test the IRF-1 mutants shown in Figure 3 (upper panel) with regard to their heterodimerization capability with ICSBP. The heterodimerization assay required DNA binding of the IRF-1 mutants. Proteins are only visible as protein–DNA complexes. Thus IRF-1 proteins, which do not bind DNA, could not be tested for heterodimerization (n.d. in Figure 3, upper panel). C-terminal deletions up to position 219 did not influence the ability of IRF-1 to heterodimerize with ICSBP (Figure 3, lower panel; lanes 7, 9 and 11). An IRF-1 mutant consisting of the N-terminal 198 amino acids still bound DNA but did not heterodimerize with ICSBP (lane 13). The same was true for more extended C-terminal deletions up to position 174 (lane 15). Another mutant of IRF-1 with an internal deletion of amino acids 190–216 did not heterodimerize (lane 36), confirming a function for heterodimerization in this region of IRF-1. Thus the C-terminal border of this association domain is between amino acids 198 and 219.

FS 143-163 is an IRF-1 mutant coding for an altered amino acid sequence between positions 142 and 164. Since this mutant still heterodimerized with ICSBP (Figure 3, lower panel; lane 28), the N-terminal border of the heterodimerization domain was presumed to be the C-terminal of position 164. These results led to the conclusion that a domain between positions 164 and 219 in IRF-1 is essential for heterodimerization with ICSBP.

Since an IRF-1 mutant with an altered amino acid composition between positions 124 and 141 did not show any heterodimerization with ICSBP, this region must contribute to heterodimerization. An IRF-1 fragment spanning amino acids 125–219 was tested in the *in vivo* two-hybrid system for sufficiency

Figure 1 Cellular distribution of IRF-1–NLS mutants

C243 fibroblasts grown on cover slips were transiently transfected with plasmids coding for the indicated proteins. Two days after transfection (**B–F**) or after fixation (**A**), living cells were examined using a fluorescence microscope with an FITC filter set. (**A**) Immunofluorescence staining (after fixation) of an IRF-1 protein which contains a C-terminal haemagglutinin tag, IRF-1–HHA [18] with the polyclonal HA.11 antibody (Hiss Diagnostics GmbH, Freiburg, Germany). (**B**) Fluorescence of wild-type IRF-1–GFP. (**C**) Fluorescence of Δbasic-GFP (Δ115-140–GFP). (**D**) Fluorescence of M6–GFP (35-329–GFP). (**E**) Fluorescence of basic-GFP (115-140–GFP). (**F**) Fluorescence of wild-type GFP.

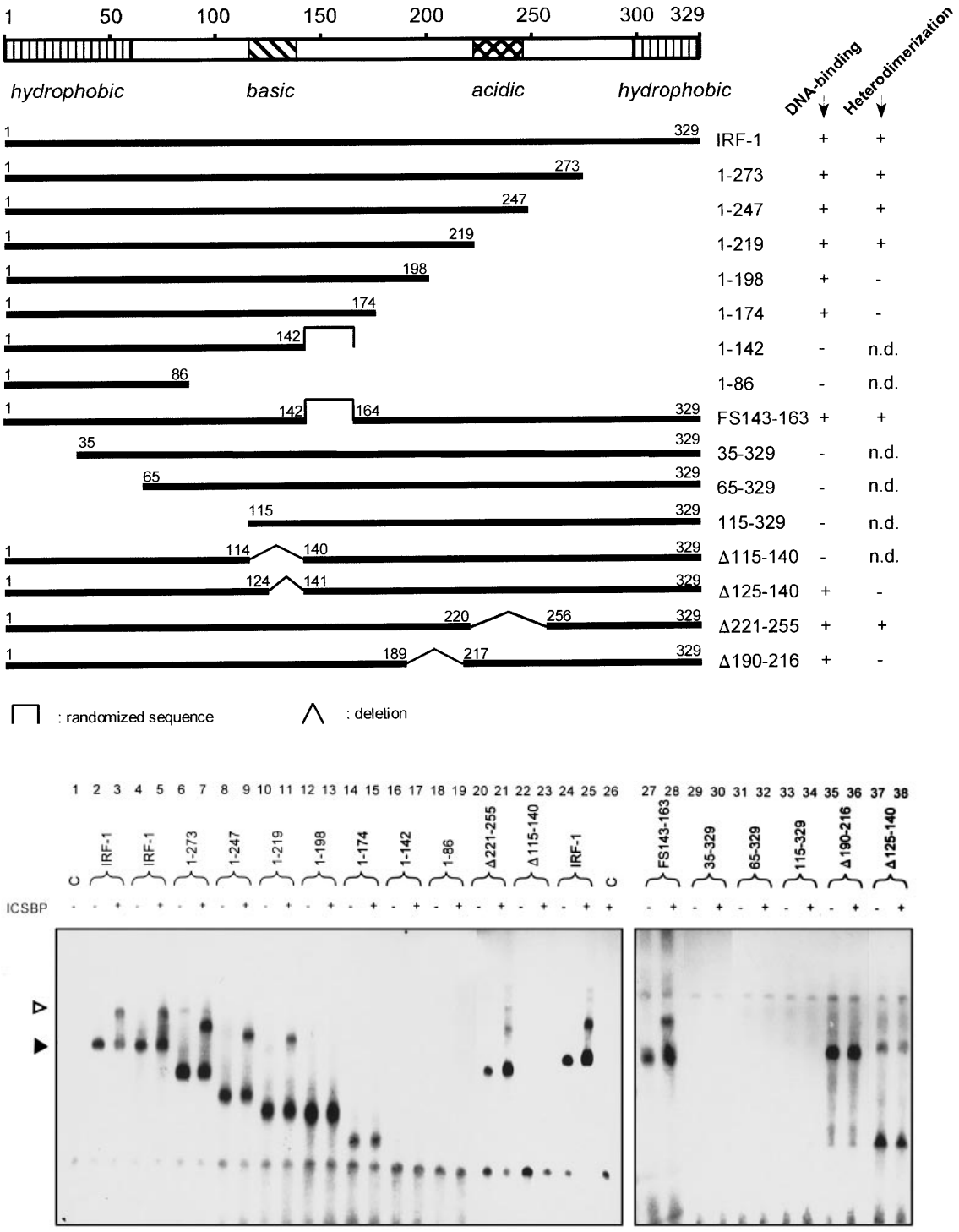

Figure 3 IRF-1 DNA binding and heterodimerization with ICSBP

Upper panel: constructs of IRF-1 mutants for DNA binding and heterodimerization (for detailed sequence information see the Experimental section). The numbers indicate the first or last corresponding amino acid in IRF-1 wild-type protein. n.d., due to lack of DNA binding, heterodimerization could not be determined. Lower panel: the indicated mutants of IRF-1 were transcribed *in vitro* and translated in rabbit reticulocyte lysates as described in the Experimental section. IRF-1, IRF-1 mutants (as indicated) or product without IRF-1 (C, lanes 1 and 26) (1 μl) was mixed with 2.5 μl of ICSBP translation product (+ICSBP) or with 2.5 μl product of a translation without RNA (−ICSBP). After 15 min incubation on ice the proteins were used for EMSA with the IFN-stimulated-gene-15–ISRE DNA fragment as described in the Experimental section. To control translation efficiency, proteins were also translated in the presence of [^{35}S]methionine and separated by SDS/PAGE. The uptake of [^{35}S]methionine in the IRF-1 mutants proteins was quantified and corrected for methionine content. The relative ratios of translation efficiency of the IRF-1 mutant proteins were as follows: IRF-1, 1.00; 1-273, 1.03; 1-247, 1.05; 1-219, 1.27; 1-198, 1.05; 1-174, 1.47; 1-142, 1.88; 1-86, 1.47; 221-255, 1.18; 115-140, 0.81; FS143-163, 0.92; 35-329, 1.05; 65-329, 1.20; 115-140, 0.81; 190-216, 1.13; 125-140, 0.81. ▷, IRF-1; ▶, IRF-1–ICSBP heterodimer.

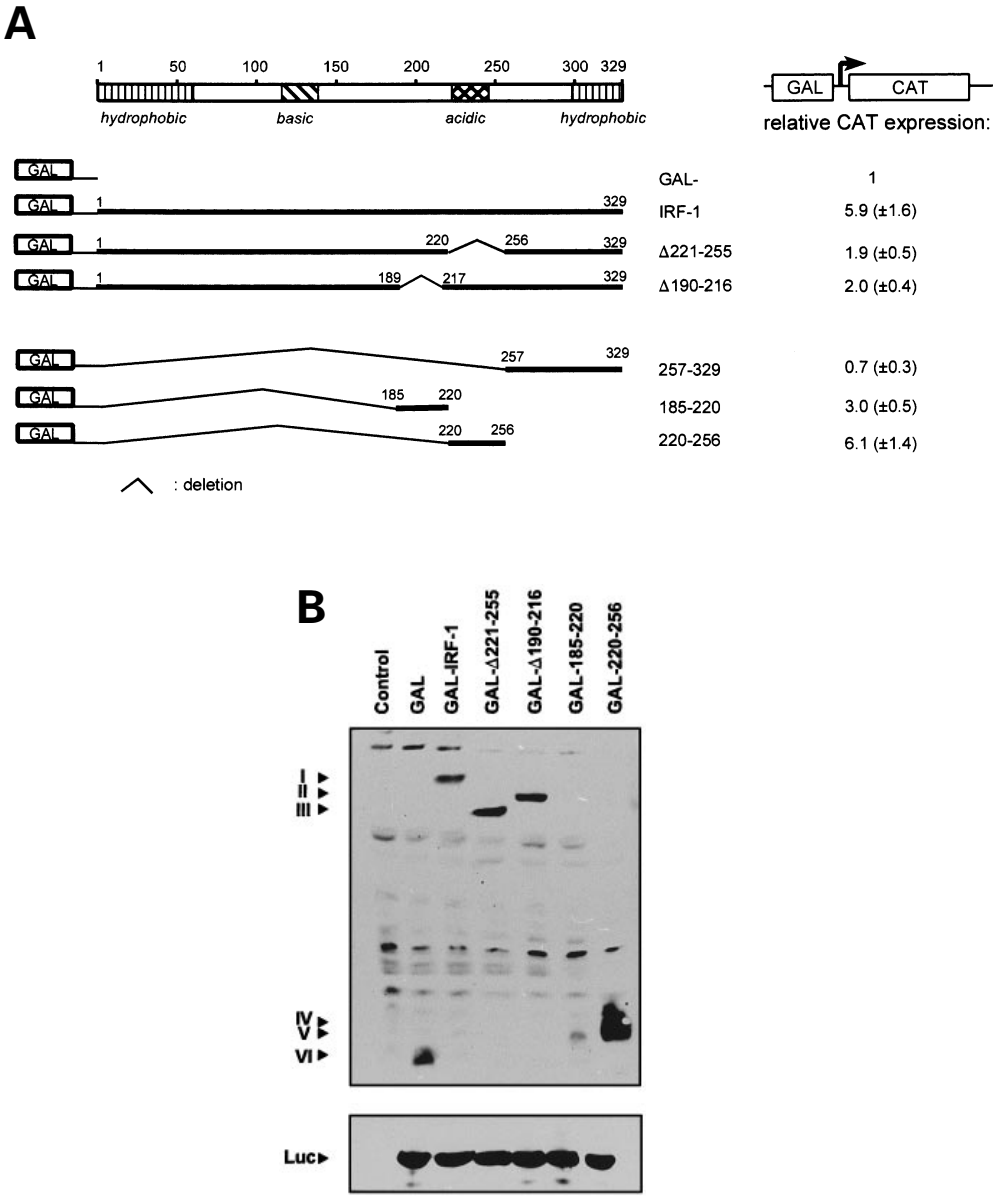

Figure 4 Transactivation of IRF-1

(**A**) Left: construction of IRF-1 mutants for transactivation assays (for detailed sequence information see the Experimental section). Deleted domains are indicated. The N-terminal fusion with the GAL4 DNA-binding domain is indicated by a rectangle. The numbers to the right indicate the first and last corresponding amino acid in the IRF-1 wild-type protein. Right: transactivation of CAT gene under control of a GAL4 responsive promoter as used for the two-hybrid assay (pMCM13). Induction levels were normalized to the corresponding control experiments with the GAL4 DNA-binding domain. Values are given as means ± S.E.M. of at least three independent experiments. (**B**) Western blot showing the levels of GAL4 and its fusion proteins (upper panel), and of luciferase, the co-transfection marker (lower panel). Cells were transfected with DNA encoding GAL4, the GAL4 fusion protein or the luciferase gene. Control cells were mock transfected. Western blots were performed with antibodies specific for GAL4 (upper panel) or luciferase (lower panel) and visualized by enhanced chemiluminescence. I, GAL–IRF-1; II, GAL–Δ190-216; III, GAL–Δ221-255; IV, GAL–220-256; V, GAL–185-220; VI, GAL; Luc, luciferase.

to heterodimerize with ICSBP. Unfortunately, this fragment alone was not sufficient to bind ICSBP (Table 1).

In this respect, the mutants shown in Figure 3 contribute to the definition of the DNA-binding domain borders of IRF-1. The N-terminal region which is conserved between all members of the IRF family enables IRF-1 to bind ISREs. Deletion of the N-terminal 34 amino acids abrogates DNA-binding activity [5] (Figure 3B, lane 30; 35-329 = M6). IRF-1 mutants with extended N-terminal deletions (65–329 and 115–329) did not bind DNA either (Figure 3B, lanes 31 and 33). This result confirms the definition of the DNA-binding domain of IRF-1 to the N-terminal part of the protein.

A C-terminal deletion of the IRF-1 protein up to position 120 leads to a loss of DNA binding [34]. An IRF-1 fragment consisting of the 150 N-terminal amino acids is able to bind the ISRE element [34]. The IRF-1 mutant Δbasic (deletion of amino acids 115–140, Figure 3, upper panel) described above was unable to bind DNA (Figure 3, lower panel, lane 22). IRF-1, with an

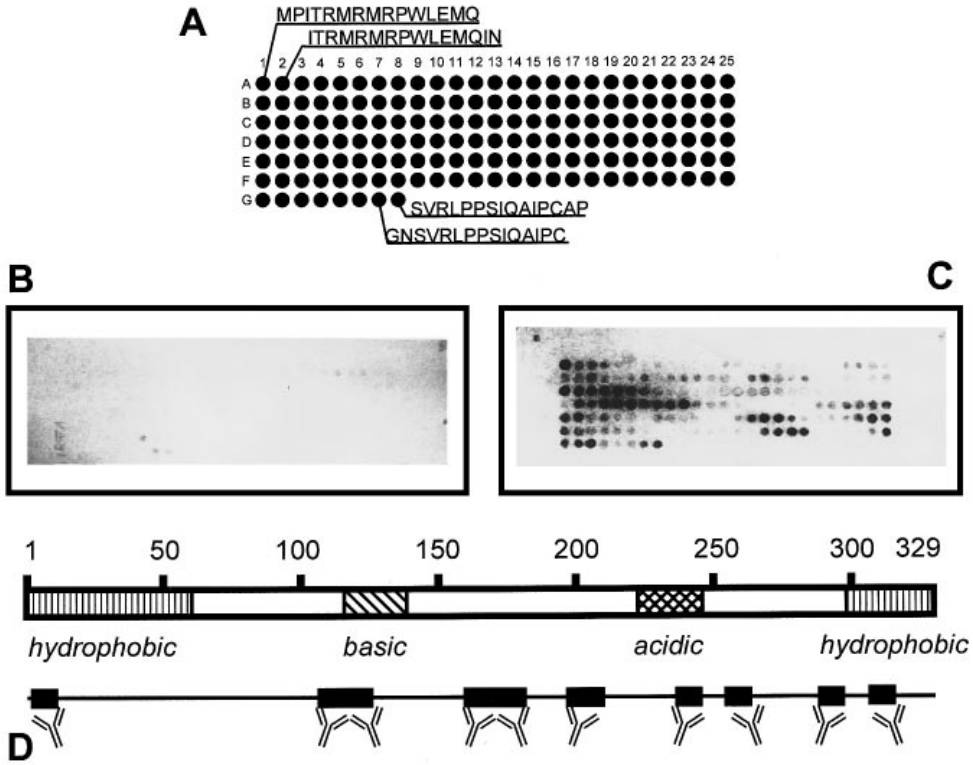

Figure 5 Exposed IRF-1 domains

(**A**) Localization of IRF-1 peptides on the membrane. Peptides corresponding to the IRF-1 amino acid sequence were synthesized and fixed at the indicated positions. All peptides contained 15 amino acids. Each of the 15-mers overlapped with 13 amino acids of the following peptide. (**B**) Binding of secondary alkaline-phosphatase-coupled antibody to the membrane. To identify non-specific binding of the secondary antibody to the IRF-1 peptides, epitope mapping without primary antibody was performed. (**C**) Epitope mapping of polyclonal antibody directed against IRF-1. (**D**) Localization of exposed epitopes in the IRF-1 protein. The identified exposed domains of the IRF-1 protein, demonstrated in (**C**) were aligned to the IRF-1 protein. The numbers indicate amino acid positions in the protein. Hydrophobic, basic and acidic domains are indicated as predicted from the primary amino acid sequence. Exposed domains are indicated by black bars bound by symbolic antibodies.

altered amino acid sequence between positions 142 and 164 (FS143-163), still bound DNA (Figure 3, lower panel, lane 28). An IRF-1 mutant lacking amino acids 125–140 possessed DNA binding activity (Figure 3, lower panel, lane 38), demonstrating that the C-terminal border did not extend beyond amino acid 125. However, an arbitrary C-terminal extension was needed to enable the fragment 1–125 to bind DNA, since amino acids 1–142 are not able to bind DNA, but mutant FS143-165 did so.

Transactivation

IRF-1 is a transcriptional transactivator. It is able to bind to TFIIB [34]. Lin et al. [34] have localized the transcriptional activation domain of IRF-1 C-terminal to amino acid 200. A cluster of acidic amino acids is located within this part of IRF-1. To determine if the acidic domain was involved in transcriptional activation, a series of deletion mutants as fusion proteins with the GAL4-DNA-binding domain was prepared (Figure 4A). The proteins were tested for induction of a GAL4-dependent CAT-reporter gene (pMCM13) in transient transfection assays with C243 fibroblasts (Figure 4A). In order to correlate the transactivation potential of the mutant GAL4 proteins with their protein level, Western blotting experiments were carried out in parallel (Figure 4B).

The wild-type IRF-1–GAL4 fusion protein induced the GAL4-responsive reporter construct about 6-fold. The same fusion protein, but with a deletion of the whole acidic domain between amino acids 220 and 256, showed a weaker transcriptional activity. A mutant with a deletion from position 190 to 216 reduced the detectable activation capacity to the same extent. This indicates the involvement of amino acids N-terminal to the acidic domain for transcriptional activation. The expression of these mutants was comparable with that of the GAL4 protein (Figure 4B). These results reveal a critical role for the domain between amino acids 190 and 255 in transcriptional activity in C243 cells. To show that the deletion of these domains within IRF-1 did not simply result in reduced transactivation due to steric alterations, a demonstration of the sufficiency of both domains for transactivation was attempted. The results depicted in Figure 4(A) further show that both domains alone are sufficient to transactivate the reporter gene. The IRF-1 protein fragment 185–220 and also the fragment 220–256 fused to the GAL4–DNA-binding domain exhibited a strong enhancement of CAT activity in the assay. The fusion protein 185–220 was less abundant (Figure 4B) and therefore the relative transactivation capacity shown in Figure 4(A) was underestimated. In contrast, the fusion protein 220–256 was more abundant than the GAL4 control, indicating that its transactivation capacity was overestimated. Nevertheless, this fusion protein showed transactivation capacity, since an increase in GAL4-encoding DNA to

Table 2 Alignment of exposed and functional domains of IRF-1

Epitopes exposed in IRF-1 protein were aligned to the identified functional domains in the protein. Numbering corresponds to the amino acid positions in wild-type IRF-1. The exposure of the identified epitopes was controlled by immunization of rabbits with corresponding synthetic peptides. The sera were tested for IRF-1 binding by EMSA [+, serum binds IRF-1–DNA complex in EMSA (supershift); −, no supershift] and immunoprecipitation (+, serum binds IRF-1 in immunoprecipitation; −, no immunoprecipitation).

Epitopes by polyclonal antibody[a]	Functional domain (mapped position in IRF-1)	Re-immunization with peptides[b]	EMSA (super-shift)	Immunoprecipitation
3–10	DNA-binding (1–125)			
105–127	Nuclear translocation (115–139)	100–125	−	−
160–180	Heterodimerization (164–219)	155–165	+	−
195–210	Heterodimerization (164–219) and transactivation (185–256)	196–217	+	+
235–242	Transactivation (185–256)	229–246	+	+
253–260	Unknown function	245–264	+	+
286–296	Unknown function	284–301	+	+
304–312	Unknown function	297–314	+	+

[a] Exposed domain as found by epitope mapping (see Figure 5C).
[b] Peptides corresponding to the indicated amino acid position in IRF-1.

achieve a similar expression level did not enhance the CAT activity from the reporter gene. The data indicate that both fragments can confer transcriptional activation to a heterologous DNA-binding protein.

Exposed IRF-1 domains

Protein domains which are responsible for protein–protein interactions are usually exposed and located on the protein surface. The protein domains which are required for nuclear translocation, heterodimerization or transactivation are candidates for such interactions.

To see whether the positions of functional domains correlated with antigenic epitopes in the IRF-1 protein, mapping was performed with a previously developed polyclonal antiserum raised against recombinant IRF-1. Using this approach, the binding of the polyclonal antibody to chemically synthesized IRF-1 peptides was tested. A number (158) of IRF-1-specific peptides, consisting of 15 amino acid residues were dotted on to a nylon membrane (Figure 5). Each of the peptides overlapped the following peptide by 13 amino acids, i.e. peptide A1 corresponded to amino acids 1–15 of IRF-1, peptide A2 corresponded to amino acids 3–17 (Figure 5A). Binding of antibodies to these peptides was visualized by the binding of a secondary alkaline-phosphatase-conjugated antibody.

The polyclonal antibody recognized peptides which corresponded to the functional domains in IRF-1. This is shown in Figures 5(C) and 5(D) and is summarized in Table 2. Some of the antigenic domains co-localized with amino acid sequences belonging to the DNA-binding domain peptides (3–10), the nuclear location signal peptides (105–127), the heterodimerization domain (160–180 and 195–210) and the transactivation domain peptides (195–210 and 235–242). In Table 2, the antigenic peptides are compared with the mapped functional domains.

To investigate whether the antigenic sites which are recognized by the polyclonal serum are exposed domains in the native IRF-1 protein, respective monospecific antibodies were created. Peptides which cover the antigenic domains were used for the immunization of rabbits. The sera were tested for the binding of IRF-1 translated in rabbit reticulocyte lysate. The binding properties of the resulting antibodies were identified by their ability to induce supershifts in EMSA (Figure 6A) and to immunoprecipitate IRF-1 (Figure 6B). To identify unspecific binding of the antibodies, the products from an *in vitro* translation without IRF-1 RNA was used in the EMSA-supershift assay

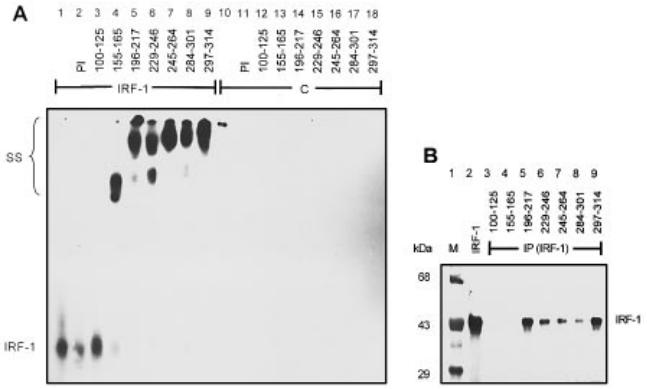

Figure 6 Antibodies from re-immunization

(**A**) IRF-1 (lanes 1–9) was translated with the rabbit reticulocyte lysate *in vitro* translation system. As a control (C) a corresponding translation was performed without IRF-1 RNA (lanes 10–18). The translation product (1 μl) was incubated with 2 μl of serum from rabbits immunized with the indicated peptides (numbering of the peptides correspond to their localization in the IRF-1 protein), with pre-immune serum (PI, lanes 2 and 11) or without addition (lanes 1 and 10) on ice for 15 min. These samples were used for EMSA with the T3 oligonucleotide as described in the Experimental section. The IRF-1–DNA complex is indicated as IRF-1, the IRF-1–antibody–DNA complex (supershift) is indicated as SS. (**B**) Sera obtained from rabbits after re-immunization with the peptides were used in immunoprecipitations. IRF-1 was translated in rabbit reticulocyte lysate in the presence of [^{35}S]methionine and 10 μl of labelled IRF-1 (lane 2) was used for immunoprecipitation with 2 μl serum of rabbits immunized with the indicated peptides [IP (IRF-1)] (lanes 3–7). M, molecular-mass standard (Gibco).

(Figure 6A, lanes 10–18). None of the antibodies caused retardation bands with the control translation products. Antibodies raised from peptides corresponding to amino acids 196–217, 229–246, 245–264, 284–301 and 297–314 in IRF-1 bound to *in vitro* translated IRF-1. The same antibodies also immunoprecipitated IRF-1.

This is strong evidence for exposure of the respective protein domains. Peptides representing sequences of the N-terminus of the heterodimerization domain (155–165) (Figure 7) induced antibodies recognizing IRF-1 in EMSA (Figure 6A, lane 4) but not in immunoprecipitation (Figure 6B, lane 4). Immunization with peptides corresponding to parts of the NLS (100–125) did not raise antibodies which bound IRF-1 in EMSA (Figure 6A, lane 3) or caused immunoprecipitation (Figure 6B, lane 3).

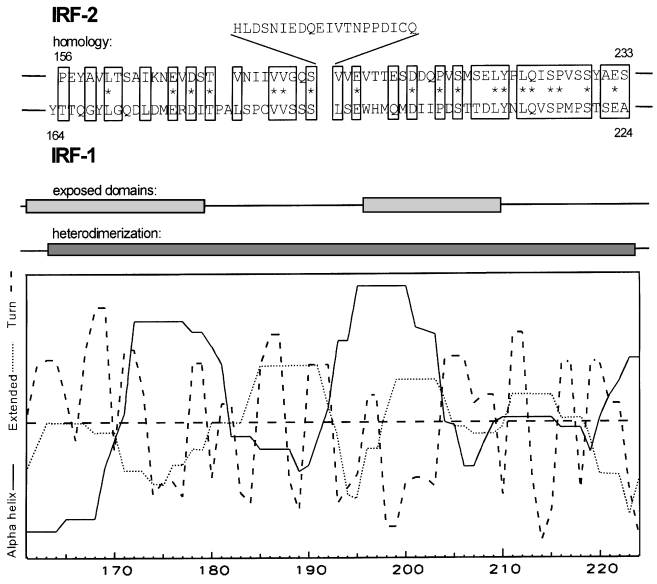

Figure 7 Heterodimerization domain of IRF-1

The heterodimerization domain of IRF-1 aligned with the amino acid sequence of IRF-2. Identical amino acids are indicated with an asterisk, similar or identical amino acids are boxed. Two exposed domains are present within this domain. Both show high helix-forming capacity as predicted from secondary structure analysis (algorithm of Robson).

DISCUSSION

In this article the different functional domains in the IRF-1 protein are described. To demonstrate nuclear localization, heterodimerization and transactivation properties *in vivo* GFP detection and a two-hybrid approach was used, thereby allowing confirmation of biochemical data published previously [32,33].

GFP was an excellent tag for the investigation of the cellular localization of IRF-1 and for showing sufficiency of a sequence as a nuclear targeting signal. This is in contrast to many other proteins, the importance in the nucleus of which is based on more than one isolated sequence. Wild-type IRF-1 protein is located in the nuclear plasma. A fusion of the NLS peptide from IRF-1 with GFP was also found in the nucleus (Figure 1E).

The *in vivo* demonstration of heterodimerization by the two-hybrid system in mammalian cells was essential to show protein–protein interaction in living cells (Table 1). Furthermore, the use of a polyclonal antipeptide antibody for defining linear epitopes on a peptide dot membrane was an essential step towards the identification of exposed surfaces of IRF-1 (Table 2).

IRF-1 is a member of a family of transcription factors. It is believed that such families develop by gene duplication and further diversification. The related part in this family concerns the N-terminal 125 amino acids of the DNA-binding domain. It contains a number of tryptophan residues at conserved positions, which seem to be essential for its tertiary structure (helix-turn-helix motif from NMR measurements reported by Uegaki et al. [36]) and the resulting DNA binding, as determined by X-ray analysis [37]. The C-terminal part does not contain an homologous sequence which is shared by all family members. According to the exon shuffling hypothesis, an evolutionary process by which new genes are generated by recombinational events to form novel combinations from pre-existing exons, the IRF-1 gene generation could be a candidate. The human gene, which is highly homologous with the mouse gene, is composed of 9 exons [38]. Exons 1, 2 and 3 (corresponding to amino acids 1–123) cover the N-terminal DNA-binding domain (amino acids 1–120), exon 4 (amino acids 124–138) contains most of the NLS (amino acids 117–141), the domain which is essential for heterodimerization (between amino acids 164 and 219) is contained in exons 5 and 6 (amino acids 139–224), mostly in exon 6, and the acidic part of the transactivation domain (amino acids 220–256) is contained in exon 7 (amino acids 225–242). Interestingly, the protein sequence encoded by exons 8 and 9 is not associated with any other known activity. Since deletions in this region do not influence any other activities, it is obvious that it does not significantly contribute to the overall IRF-1 structure. We speculate that other activities, such as surfaces to interact with heterologous proteins are contained within this region. For example, it was shown that members of the nuclear factor-κB/rel family bind to IRF-1 [39].

From the above one could assume that IRF-1 is a typical modular protein, the overall structure of which is not relevant to the function of the individual domains. Indeed, it is possible to functionally translocate the DNA-binding domain [40,41], the transcriptional activation domain and the NLS to other proteins. A mutual influence of the domains with the test systems presented in the present work was not observed. Since we were not able to show sufficiency of the 'heterodimerization domain' to ICSBP after fusion to heterologous proteins we assume that additional sequences or structures outside of the essential part exist. It is also possible that this function requires a conformational structure. Although we could not find a canonical nuclear export sequence within IRF-1, we cannot exclude the existence of an export signal. While IRF-3 contains a nuclear export sequence [13], the requirement for such a signal in IRF-1 is not obvious.

Sequence similarity of IRF-1 to IRF-2 in the parts C-terminal to the DNA-binding domain is of particular interest. IRF-2, which is thought to reside in the nucleus, should also have (a) NLS sequence(s). A basic amino acid sequence is found at the respective position to the NLS in IRF-1. Ten of the 12 basic amino acid residues in IRF-1 are found at identical positions in IRF-2. This suggests the same role as in IRF-1.

The amino acid sequence of the heterodimerization domain of IRF-1 is conserved in IRF-2, but IRF-2 contains a 13 amino acid insertion within this domain (Figure 7). IRF-2 heterodimerizes with ICSBP with an even higher affinity. It is possible that this insertion is responsible for the enhanced affinity. In this respect, it is of interest to note that IRF-2 (positive regulatory domain I-BFc) is cleaved upon virus induction [13,42]. This cleavage site is exactly at the N-terminal border (amino acid 164) of the respective region of the heterodimerization domain in IRF-1. The remaining N-terminal part of IRF-2 (positive regulatory domain I-BFi) should therefore not be able to bind to ICSBP.

We thank R. Frank for helpful discussions, Dr. J. Chebath (Weizmann Institute of Science, Rehovot, Israel) for the polyclonal antibody raised against recombinant IRF-1, Dr. M. Ptashne (Harvard University, Boston, MA, U.S.A.) for the plasmids pSGVP and pSG424, Dr. I. Haviv (Weizmann Institute of Science, Rehovot, Israel) for the polyclonal antibody directed against GAL4 and R. Avram for typing the manuscript. This work was supported by the German-Israeli Foundation for Scientific Research and Development (Research Grant No. I 0247-110.02/92).

REFERENCES

1 Fujita, T., Sakakibara, J., Sudo, Y., Miyamoto, M., Kimura, Y. and Taniguchi, T. (1988) EMBO J. **7**, 3397–3405
2 Kirchhoff, S., Koromilas, A. E., Schaper, F., Grashoff, M., Sonenberg, N. and Hauser, H. (1995) Oncogene **11**, 439–445
3 Miyamoto, M., Fujita, T., Kimura, Y., Maruyama, M., Harada, H., Sudo, Y., Miyata, T. and Taniguchi, T. (1988) Cell **54**, 903–913
4 Pine, R., Decker, T., Kessler, D. S., Levy, D. E. and Darnell, Jr., J. E. (1990) Mol. Cell. Biol. **10**, 2448–2457

5 Kirchhoff, S., Schaper, F. and Hauser, H. (1993) Nucleic Acids Res. **21**, 2881–2889
6 Tamura, T., Ishihara, M., Lamphier, M. S., Tanaka, N., Oishi, I., Aizawa, S., Matsuyama, T., Mak, T. W., Taki, S. and Taniguchi, T. (1995) Nature (London) **376**, 596–599
7 Tanaka, N., Ishihara, M., Kitagawa, M., Harada, H., Kimura, T., Matsuyama, T., Lamphier, M. C., Aizawa, S., Mak, T. W. and Taniguchi, T. (1994) Cell **77**, 829–839
8 Harada, H., Fujita, T., Miyamoto, M., Kimura, Y., Maruyama, M., Furia, A., Miyata, T. and Taniguchi, T. (1989) Cell **58**, 729–739
9 Tanaka, N., Ishihara, M., Lamphier, M. S., Nozawa, H., Matsuyama, T., Mak, T. W., Aizawa, S., Tokino, T., Oren, M. and Taniguchi, T. (1996) Nature (London) **382**, 816–818
10 Nelson, N., Marks, M. S., Driggers, P. H. and Ozato, K. (1993) Mol. Cell. Biol. **13**, 588–599
11 Weisz, A., Kirchhoff, S. and Levi, B.-Z. (1994) Int. Immunol. **6**, 1125–1131
12 Weisz, A., Marx, P., Sharf, R., Appella, E., Driggers, P. H., Ozato, K. and Levi, B.-Z. (1992) J. Biol. Chem. **267**, 25589–25596
13 Yoneyama, M., Suhara, W., Fukuhara, Y., Fukada, M., Nishida, E. and Fujita, T. (1998) EMBO J. **17**, 1087–1095
14 Driggers, P. H., Ennist, D. L., Gleason, S. L., Mak, W.-H., Marks, M. S., Levi, B.-Z., Flanagan, J. R., Appella, E. and Ozato, K. (1990) Proc. Natl. Acad. Sci. U.S.A. **87**, 3743–3747
15 Sharf, R., Azriel, A., Lejbkowicz, F., Winograd, S. S., Ehrlich, R. and Levi, B.-Z. (1995) J. Biol. Chem. **270**, 13063–13069
16 Bovolenta, C., Driggers, P. H., Marks, M. S., Medin, J. A., Politis, A. D., Vogel, S. N., Levy, D. E., Sagakuchi, K., Appella, E., Coligan, J. E. and Ozato, K. (1994) Proc. Natl. Acad. Sci. U.S.A. **91**, 5046–5050
17 Sharf, R., Merado, D., Azriel, A., Thornton, A. M., Ozato, K., Petricoin, E. F., Larner, A. C., Schaper, F., Hauser, H. and Levi, B.-Z. (1997) J. Biol. Chem **272**, 9785–9792
18 Holtschke, T., Löhler, J., Kanno, Y., Fehr, T., Giese, N., Rosenbauer, F., Lon, J., Knobeloch, K.-P., Gabriele, L., Waring, J. F., Bachmann, M. F., Zingernagel, R., Morse, III, H. C., Ozato, K. and Horak, I. (1996) Cell **87**, 307–317
19 Sambrook, J., Fritsch, E. F. and Maniatis, T. (1989) in Molecular Cloning: A Laboratory Manual, Cold Spring Harbor Laboratory, Cold Spring Harbor, New York
20 Dirks, W., Schaper, F. and Hauser, H. (1994) Gene **149**, 389–390
21 Dirks, W., Schaper, F., Kirchhoff, S., Morelle, C. and Hauser, H. (1994) Gene **149**, 387–388
22 Sadowski, I., Ma, J., Triezenberg, S. and Ptashne, M. (1988) Nature (London) **335**, 563–564
23 Artelt, P., Morelle, Ch., Ausmeier, M., Fitzek, M. and Hauser, H. (1988) Gene **68**, 213–219
24 Fried, M. and Crothers, D. M. (1981) Nucleic Acids Res. **9**, 6505–6525
25 Frank, R. (1992) Tetrahedron Lett. **48**, 9217–9232
26 Laemmli, U. K. (1970) Nature (London) **227**, 680–685
27 Oie, H. K., Gazdar, A. F., Buckler, C. E. and Baron, S. (1977) J. Gen. Virol. **1**, 107–109
28 Zawatzky, R., De Maeyer, E. and De Maeyer-Guignard, J. (1985) Proc. Natl. Acad. Sci. U.S.A. **82**, 1136–1140
29 Graham, F. and van der Eb, L. (1973) Virology **52**, 456–487
30 de Wet, J. R., Wood, K. V., DeLuca, M., Helinski, D. R. and Subramani, S. (1987) Mol. Cell. Biol. **7**, 725–737
31 Garcia-Bustos, J., Heitman, J. and Hall, M. N. (1991) Biochim. Biophys. Acta **1071**, 83–101
32 Cubitt, A. B., Heim, R., Adams, S. R., Boyd, A. E., Gross, L. A. and Tsien, R. Y. (1995) Trends Biochem. Sci. **20**, 448–455
33 Thaku, S., Zhang, B. H., Peng, Y., Le, H., Carroll, B., Ward, T., Yao, J., Farid, L. M., Couch, F. J., Wilson, R. B. and Weber, B. (1997) Mol. Cell. Biol. **17**, 444–452
34 Lin, R., Mustafa, A., Nguyen, H., Gewert, D. and Hiscott, J. (1994) J. Biol. Chem. **269**, 17542–17549
35 Reference deleted
36 Uegaki, K., Shirakawa, M., Harada, H., Taniguchi, T. and Kyogoku, Y. (1995) FEBS Lett. **359**, 184–188
37 Escalaute, C. R., Yie, J., Thanos, D. and Aggariwal, A. K. (1998) Nature (London) **39**, 103–106
38 Cha, Y., Sims, S. H., Romine, M. F., Kaufmann, M. and Deisseroth, A. B. (1992) DNA Cell Biol. **11**, 605–611
39 Drew, P. D., Franzoso, G., Becker, K. G., Bours, V., Carlson, L. M., Siebenlist, U. and Ozato, K. (1995) J. Interferon Cytokine Res. **15**, 1037–1045
40 Fujita, T., Kimura, Y., Miyamoto, M., Barsoumian, E. L. and Taniguchi, T. (1989) Nature (London) **337**, 270–272
41 Harada, H., Kitagawa, M., Tanaka, N., Yamamoto, H., Harada, K., Ishihara, M. and Taniguchi, T. (1993) Science **259**, 971–974
42 Whiteside, S. T., King, P. and Goodbourn, S. (1994) J. Biol. Chem. **269**, 27059–27065

Received 5 January 1998/5 June 1998; accepted July 28 1998